Spatial and Temporal Analysis of Traffic States on Large Scale Networks

Cyril Furtlehner, Yufei Han, Jean-Marc Lasgouttes, Victorin Martin, Fabrice Marchal, Fabien Moutarde

Spatial and Temporal Analysis of Traffic States on Large Scale Networks

Cyril Furtlehner*, Yufei Han†, Jean-Marc Lasgouttes*, Victorin Martin*, Fabrice Marchal‡, Fabien Moutarde†
* INRIA, France – email: firstname.lastname@inria.fr
† Robotics Lab (CAOR), Mines-ParisTech, France – firstname.lastname@mines-paristech.fr
‡ AXONACTIVE AG, Switzerland – firstname.lastname@axonactive.com

***Abstract*— We propose a set of methods aiming at extracting large scale features of road traffic, both spatial and temporal, based on local traffic indexes computed either from fixed sensors or floating car data. The approach relies on traditional data mining techniques like clustering or statistical analysis and is demonstrated on data artificially generated by the mesoscopic traffic simulator Metropolis. Results are compared to the output of another approach that we propose, based on the belief-propagation (BP) algorithm and an approximate Markov random field (MRF) encoding on the data. In particular, traffic patterns identified in the clustering analysis correspond in some sense to the fixed points obtained in the BP approach. The identification of latent macroscopic variables and their dynamical behavior is also obtained and the way to incorporate these in the MRF is discussed as well as the setting of a general approach for traffic reconstruction and prediction based on floating car data.**

I. Introduction

With the development of telecommunication networks, is has become possible to collect floating car data, coming directly from the vehicles embedded in traffic, either from mobiles traces [1] or directly from specially equipped vehicles [2]. Once those data are acquired, it remains to incorporate them in models able not only to complete or correct the traffic description, but also to predict short term future traffic. Traditional methods rely on traffic models (see e.g. [3], [4] for a review), where a few parameters have to be calibrated based on rather homogeneous assumptions and on few observations. Intermediate kinetic descriptions including cellular automata [5] are instrumental for powerful simulation and prediction systems in equipped road networks [6]. Data driven approaches, which have become more and more popular because of the sharp increase of available data, mainly use statistical dependencies combined with various techniques of artificial intelligence [7], [8], while global prediction systems on a network combine data analysis and model simulations [6], [9]. Notably, few studies, mainly based on multivariate analysis (e.g. [10], [11]), try to mix spatial and temporal dependencies, possibly because most methods do not scale well with the size of traffic networks under real-time constraints.

In a preceding work [12], we proposed a method based on the Belief-Propagation algorithm (BP) [13], to overcome the scalability problem. The basic idea is to encode the spatial and temporal dependencies into an approximate MRF calibrated directly by constraining the output of BP. This approach is now is at the core of the Field Operational Test project Pumas[1], in which a thousand of vehicles will be fitted with a custom-made on-board unit, in order to do traffic reconstruction and prediction in the urban agglomeration of Rouen (Normandy). The idea is to gather floating car data (FCD) sent by these probe vehicles and to build a Markov Random Field which models the statistical interaction between the road segments. Then, in operating conditions, the data that arrives in real-time is propagated in time and space using the BP algorithm (see [12] and Section IV for more details). This approach is particularly well suited to medium-sized cities, which do have congestion problems, but cannot afford to invest in magnetic loops to sense the traffic in the whole city.

It is difficult however to understand the structure of the traffic correlations in a city without real FCDs. Therefore, a first step is to test our ideas on synthetic data coming from the mesoscopic simulator Metropolis. The goal is not to calibrate a model usable in a real urban environment, but to see how much of the simulated output we can predict or reconstruct.

Statistical and data mining analysis is crucial for understanding the kind and amount of information contained in the data, which range from local correlation due to diffusion of congestion on the network, to large scale traffic patterns and their dynamical behavior. Once large scale structures are identified, we can see whether they are recovered with BP or, alternatively, how to incorporate them as extra knowledge in the model. The purpose of the present paper is to elucidate this question. It organized as follows: in Section II we describe the traffic simulator and the database we use for experimenting our techniques; Section III is devoted to various clustering tests on the data to identify spatial and temporal traffic patterns. In Section IV, after recalling our approach based on BP, we analyze the fixed point structure which is obtained by running BP on these data. Finally, in Section V, we compare results of Sections III and IV.

II. Metropolis and the artificial database

A. Metropolis

Metropolis [14], [15] is a planning software dedicated to the modeling of transportation systems. It is a unique tool that allows to study the impacts of transportation policies for metropolitan areas and their fringes in a time-dependent framework. This software proposes a complete environment to handle dynamic simulations of car traffic, it is intended

[1] see http://pumas.inria.fr/ for a description (in French)

for the planning and for the management of large to very large urban transportation networks.

B. Sioux Falls and Paris region based networks

The Metropolis databases that we use in this study are structured as follows.

1) The supply: from the economic viewpoint, the traffic network constitutes the supply to the agents, i.e. the resource that the single car driver has to compete for. To build the benchmark database on which we want to test and analyze our methods at first, we have chosen the classic small scale traffic network Sioux Falls [16] and a large scale one, based on the Paris and suburbs network. The first one consists of 23 intersections and 110 segments, while the second one is composed 4660 intersections and 13625 segments.

2) The demand: The basic requirements of each agent in the Metropolis system is to perform a pre-defined trip between a specific origin and a specific destination. Agents maximize a utility function that includes travel time, schedule delay costs as well as potential tolls. A coarse grained description of the aggregate demand is provided by a set of calibrated Origin-Destination (O-D) matrices, For Sioux Falls, the number of simulated agents is of the order of $3 \cdot 10^5$, while it is of the order of $3 \cdot 10^6$ for Paris and suburbs.

3) Traffic situations: they are obtained through random events and fluctuation in supply and demand. Each simulated traffic situation that we use covers 8 hours of a morning congestion. Different scenarios are predefined to vary the demand, through the global intensity of the main components of the O-D matrix, and the supply, through the capacity of network flow. For Sioux Falls, our database comprises a total of 107 different traffic situations of 36 time steps each, while for Paris and suburbs there 108 scenarios of 48 time steps each. The time steps correspond to 15-minute bins over which network performances were aggregated over time.

4) The data output: all travel times for each segment at any time are converted into a traffic index

$$x_{\ell t} \stackrel{\text{def}}{=} \frac{\Delta t^0_\ell}{\Delta t_{\ell t}} \in [0,1], \tag{1}$$

where Δt^0_ℓ is the free-flow travel time on segment ℓ and $\Delta t_{\ell t}$ the observed one at time t. $x_{\ell t} = 1$ corresponds to free flow while lower values indicate congestion. Spatial average of this index yields the global traffic index, indicating the overall congestion level on the network.

III. Statistical analysis of the data

A. Generalities

Clustering analysis is an intuitive way for digging out statistical characteristics of traffic dynamics within local neighborhoods or over the whole network from massive traffic data. Through the statistical procedure, we can describe latent temporal and spatial correlations of traffic states among different links quantitatively, which can be used to place additional constraints on the random field based model of Section IV, or to assess the validity of model assumptions. In this section, we perform clustering analysis in two respects. For one thing, we group links according to their temporal dynamics. Exemplars of resultant groups reveal representative link dynamic patterns. Links within the same groups are inclined to have similar temporal behaviours in a statistical sense. For another thing, we perform clustering procedure to obtain typical spatial layouts of traffic states in the whole network, which represent spatial constraints of congestion level between different links.

A common approach in clustering analysis is to learn cluster centroids by iteratively decreasing the sum of squared errors between data points and their nearest centroids. The popular K-means algorithm [17] follows this idea. However, it suffers from sensitivity to initialization of exemplars and implicit assumption of spherical cluster shapes. It is necessary to run K-means with several random initializations to get satisfactory cluster structures. In our application, we hardly have any prior knowledge about underlying traffic data distributions before clustering. Therefore, we adopt a local message-passing-based clustering approach, named affinity propagation, which was firstly proposed by Frey and Dueck in [18]. This algorithm takes all data points as candidates of representative "exemplars". Two scalar messages, "availability" and "responsibility" noted respectively a_{ik} and r_{ik} are transmitted between data point i and k as follows:

$$r(i,k) \leftarrow s(i,k) - \max_{k' \neq k} \big\{ a(i,k') + s(i,k') \big\} \tag{2}$$

$$a(i,k) \leftarrow \min \Big[0, r(k,k') + \sum_{i' \notin \{i,k\}} \max\{0, r(i',k)\} \Big] \tag{3}$$

$s(j,k)$ is the similarity measure between data points j and k, defined as the negative euclidean distance in our work. The messages measure accumulated evidences of the assumption that k is the exemplar of i. Through iteratively transmitting and updating of scalar valued messages, a proper setting of exemplars can be obtained. The stopping criteria for the iterative procedure is that exemplar decisions do not change for iterations of specific amounts. Using affinity propagation based clustering, we firstly achieve a stable optimal solution to the setting of exemplars by adjusting the stopping criteria, which prefers small number of clusters. Afterwards, we traverse two neighboring suboptimal solutions that get successively larger numbers of clusters than the optimal choice to describe details about cluster structures.

B. Clustering roads according to temporal behaviours

To group links, we concatenate traffic indices of each link into a vector. Components in each vector are arranged according to their temporal orders in different simulations. In our work, we make use of 107 different simulations. Each one contains traffic indices of 72 links sampled at 36 time steps within the same day. Thus, the dimension in each link vector is $36 \times 107 = 3852$. Such vectors describe temporal dynamics of corresponding links. Fig. 1 illustrates the optimal and two sub-optimal settings of cluster structures. We show proportions of each cluster and temporal behaviors of exemplars in the figure. Because we focus on daily temporal dynamics of links in this paper, we use average of traffic index sequences in the

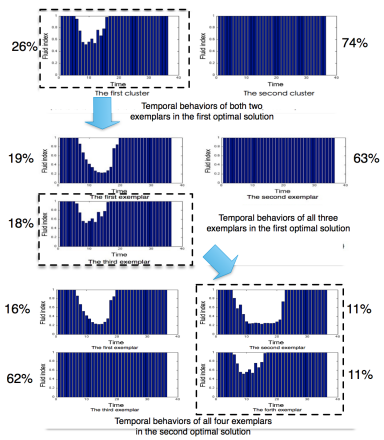

Fig. 1. Hierarchical division of cluster structures

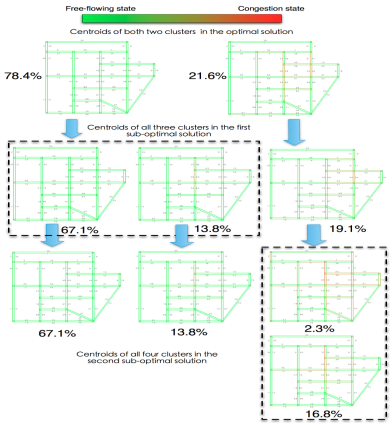

Fig. 2. Hierarchical division of global traffic states

same cluster as the exemplar of link dynamics. According to the figure, the cluster structures in the sub-optimal solutions split the optimal cluster structure hierarchically, which refines information of link temporal dynamics.

As we can see, the optimal clusters represent two typical link dynamics. The first one corresponds to emergence of congestion during early in daytime, while the second one denotes free flowing through the whole day. Over 70% of the links are free from jam in most of situations. In a further step, the first cluster in the optimal setting is further divided into two sub-groups in the first sub-optimal solution. Due to existence of sparsely distributed data points that can not get stable assignment, the division relation can not be measured exactly. Nevertheless, the membership between link groups is distinct. The optimal cluster structure only denotes presence or absence of congestion in daily link dynamics. Exemplars of the first and third cluster in the first sub-optimal solution refine temporal patterns of link dynamics with occurrence of congestion, which corresponds to traffic jam of severe and medium level respectively. Moreover, the third cluster is further partitioned into two sub-clusters in the second sub-optimal cluster. They represent different congestion durations. With increasing numbers of cluster centers, details of obtained temporal behavior patterns become more and more abundant.

C. Unveiling typical spatial patterns by clustering global network states

To group global traffic patterns, we arrange traffic indices of all 72 links sampled at the same time step in each simulation into a vector according to spatial locations, which lies in a $\mathbb{R}^{72}$ feature space. As there are 107 simulations, there are a total of 3852 feature vectors as training data of clustering. Resultant exemplars of clusters represent typical spatial configurations of global traffic status. To illustrate the spatial configurations intuitively, we project traffic indices of links to a continuous colour map in Fig. 2. Gradual variations of colour from green to red correspond to traffic states of links varying from free-flowing to congestion. The optimal solution involves two clusters. The first exemplar denotes that all links are fluid, while the link network falls into traffic jam in the second exemplar. They can only provide a profile of global traffic status. By increasing exemplars in the sub-optimal solutions, the two clusters are partitioned into subsets in a hierarchical way. Based on new exemplars emerged from hierarchical division, we derive refined descriptions of spatial configurations of traffic flows. According to Fig. 2, the free-flowing cluster is split into two sub-clusters in the first sub-optimal solution. They correspond to an overall fluid state and a intermediate state that represents short-term transition from free-flowing to congestion or vice versa. Through further division of cluster structures in the second optimal solution, we can identify patterns of spatial configurations in the third and forth exemplar. Notably, the free-flowing state has the largest proportion among clusters. It indicates that the network is fluid in most situations.

D. Temporal dynamics of global network

We inspect temporal behaviors of the global network through its transition between traffic patterns identified in III-C. For each time step, we take average of traffic indices in each link in different simulation groups. Afterwards, we assign each 72 dimensional vector of average traffic indices into clusters obtained in the optimal and sub-optimal solutions of affinity propagation, which corresponding typical global traffic patterns. Fig. 3 illustrates daily temporal evolution of the global patterns. Green, blue and red bars correspond to free-flowing, intermediate and congestion state respectively. Cyan and purple bars represent medium and severe congestion state in the second sub-optimal clustering solution. Lengths of bars measure duration of the patterns in the temporal sequences. According to Fig. 3, the link network is always congested at the start of one day. Then it recovers soon to be fluid. Free-flowing and congestion are two common statuses of the whole network, while the intermediate state is just a short transition between them. Thus, intermediate states could be used to predict emergence of congestion or aiding BP as latent variables. Furthermore, with hierarchical division of clusters, we could observe increasingly finer details about transition of states, which depicts temporal dynamics elaborately. In this figure, we also compare the temporal evolution of global states

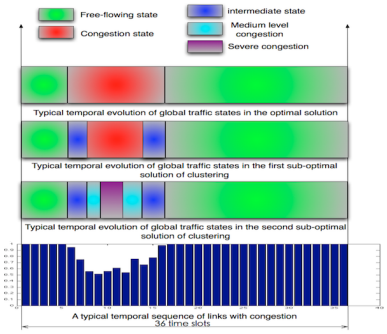

Fig. 3. A typical temporal evolution of global traffic states

to a typical temporal link behavior with the same sampling scale. Apparently, no matter how many clusters we obtain, there is a consistent correspondence between the time when congestion of single links and the whole network emerges or disappears. It denotes correlation between traffic states of individual links and the whole network.

IV. The Belief-Propagation Approach

A. Building the model

The use of message passing algorithms in the context of traffic prediction is in some sense dictated by real-time data processing requirements. The method proposed in [12], after discretization of the network in segments and discretization of time in slots of, say, 15 minutes, is firstly based on an abstract encoding of the traffic data. We define a set of local binary indexes $\tau_{\ell t} \in \{0,1\}$, indicating whether segment ℓ at discrete time t is congested ($\tau_{\ell t}=0$) or fluid ($\tau_{\ell t}=1$). Then $x_{\ell t}$, as defined in (1), is interpreted as the probability of $\tau_{\ell t}=1$. The algorithm will return *in fine* the probabilities of τ being 1, which can be interpreted back as travel time predictions, after inverting the historical data distribution of local traffic indexes.

Given this encoding, the data collected from the probe vehicles over long periods (weeks or months) are used to build an historical database, in the form of a set of single and pairwise empirical marginals of the generic type,

- $\hat{p}_\ell(\tau_\ell)$: the probability that segment ℓ is in state τ_ℓ;
- $\hat{p}_{\ell\ell'}(\tau_\ell,\tau_{\ell'})$: the probability that a pair of segments (ℓ,ℓ') find itself in the joint state $(\tau_\ell,\tau_{\ell'})$.

Note that purely spatial dependencies are considered here for sake of notational simplicity, but in practice we are interested to combine both spatial and temporal dependencies, since vehicles move both in space and time. To avoid specifying this, let us simply denote from now on by i the variable index, which is either a spatial ℓ or a combination (ℓ,t) of spatial and temporal indexes. These dependencies can be graphically summarized into a graph (explained in the next Section) where the set of vertices is $\mathcal{V}=\mathcal{L}\otimes\mathcal{T}$, with $\mathcal{L}$ corresponding to the segments of the original traffic network and $\mathcal{T}$ is the discrete set of time slots. Each edge $(i,j)\in\mathcal{E}$ connecting two nodes (i,j) of the graph $\mathcal{G}$ is then reflecting an explicit dependency $\hat{p}_{ij}$ between these nodes.

For some reasons exposed in [19], the best choice of joint distribution knowing $\hat{p}$ is of the form

$$P(\{\tau\}) = \prod_{(i,j)\in\mathcal{E}} \psi_{ij}(\tau_i,\tau_j) \prod_i \phi_i(\tau_i), \tag{4}$$

where we propose to define

$$\psi_{ij}(\tau_i,\tau_j) = \Big(\frac{\hat{p}_{i,j}(\tau_i,\tau_j)}{\hat{p}_i(\tau_i)\hat{p}_j(\tau_j)}\Big)^\alpha, \qquad \phi_i(\tau_i)=\hat{p}_i(\tau_i).$$

In the definition above, $0\leq\alpha\leq 1$ a real parameter, which aims at compensating the amplification of some interactions, created by cycles in the graph. We rely here on a single parameter although a more refined multi-parameter version has been considered in [19]. Let us emphasize also here that the choice of the edges (i,j) is not a prior, but is data driven, depending on the most significant dependencies obtained from the floating car data.

The joint-measure (4) can be conveniently pictured with a a so-called factor-graph, which somehow represents the communication network on which messages are exchanged, and various topologies may be associated to different inference schemes. To design it we proceed as follows: from the historical data, we compute the mean traffic index distribution corresponding to the spatial configurations. This mean index is obtained for each simulation and each time slot by averaging over the links the local traffic index (1). Reverting this distribution, for each segment of the network, we then compute its mean traffic index and the corresponding variance with respect to the uniform measure of mean traffic indexes. This allows to filter out the free-flow configurations.

B. The BP algorithm

The belief propagation algorithm [13] is an iterative distributed procedure, exact on a graph with no loops, able to approximate all single and pairwise marginals (associated to $\mathcal{E}$) of the joint measure (4). The basic entities subject to recursive update are messages exchanged between variables: if $(i,j)\in\mathcal{E}$, the message $m_{ij}(\tau_j)$ sent by i to j depends one the state of j. The update of the messages takes the following form in our case:

$$m_{ij}(\tau_j) \propto \sum_{\tau_i\in\{0,1\}} \psi_{ij}(\tau_i,\tau_j)\phi_i(\tau_i) \prod_{k\in j\setminus i} m_{ki}(\tau_i), \tag{5}$$

where the $\propto$ symbol indicates that $m_{ij}(0)+m_{ij}(1)=1$ and $k\in i$ denotes graph neighbouring of i. The single variable beliefs, which are the approximations of the marginal distribution of each τ_i, read

$$b_i(\tau_i) \propto \phi_i(\tau_i) \prod_{j\in i} m_{ji}(\tau_i).$$

In absence of information, one expects to recover historical data: $b_i(\tau_i)=\hat{p}(\tau_i)$. In fact, this is supposed to be the the case only when $\alpha=1$. Even in this case, this fixed point which always exists is not necessarily stable, and instead the procedure may converge toward some other fixed point. As observed in [19], if a certain number of sufficiently distinct traffic states are present in the underlying distribution,

they will be reflected as belief-propagation fixed points or equivalently as minimum of the associated Bethe free energy [20], when the parameter α is correctly adjusted.

C. Inserting real time information

We tackle here the problem of including the real time information x_i^* obtained from floating car data into the BP model. To this end, we define the probability distribution

$$p_i^*(\tau_i) \stackrel{\text{def}}{=} \tau_i x_i^* + \bar{\tau}_i(1 - x_i^*)$$

The heuristic proposed in [12] consists in giving a bias $p_i^*/\hat{p}_i$ to the messages originating from a variable i for which information is provided. More precisely, the message sent by such a node i to a neighbor node j is not computed by (5) anymore, but becomes

$$m_{ij}(\tau_j) \propto \sum_{\tau_i \in \{0,1\}} \psi_{ij}(\tau_i, \tau_j) p_i^*(\tau_i) \prod_{k \in j \setminus i} m_{ki}(\tau_i). \qquad (6)$$

In statistical physics parlance, one would say that this heuristic includes the real time information in the local fields. It allows to reconstruct the traffic state, up to some noise, better and better as the percentage of known nodes states increases (see the decimation results in [19]), but it lacks a theoretical basis. Following [20], which shows that Belief Propagation is an iterative solution to a minimization problem, we can define a new minimization problem imposing that $b_i = p_i^*$ at nodes i where the ratio x_i^* is known. The solutions to this optimization problem are fixed points of the following message updates: for each node i where we know p_i^*, we replace (5) with

$$m_{ij}(\tau_j) \propto \sum_{\tau_i \in \{0,1\}} \psi_{ij}(\tau_i, \tau_j) \frac{p_i^*(\tau_i)}{m_{ji}(\tau_i)} \qquad (7)$$

To test this new scheme, 200 spatial configurations are randomly selected from the historical database, and gradually the actual values x_i^* of some variables are revealed, varying the density ρ of revealed variables from 0 to 1; then, for different values of α, BP is run according to the prescriptions (6) and (7). The mean reconstruction error is computed as the mean over the set $\mathcal{V} \setminus \mathcal{V}^*$ of unknown variables of $|x_i^* - b_i(1)|$, averaged oven the sample data. An integrated reconstruction performance measure is additionally defined, by summing over values of ρ (see next section).

Fig. 4 shows that (7) is a more precise and theoretically sound way of inserting real time information in our BP schema. Moreover, the historical data-based prediction error, which is the absolute difference between the observed traffic index in the spatial sample and the historical mean traffic index at that time has been added to Fig. 4. It shows that, even for the very noisy data of Sioux Falls, both BP-based approaches yield a sensibly better information than simple time dependent historical data, as soon as $\rho \geq 0.1$.

D. Fixed point analysis as a clustering method

The different belief propagation fixed points obtained in absence of day-time information by varying messages initializations, represent in principle the various traffic macro-states that can be observed. It is therefore interesting to compare them with the results of the statistical analysis performed in Section III.

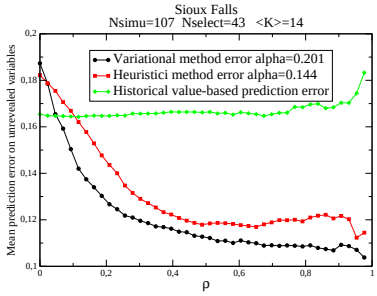

Fig. 4. Comparison of the two proposed methods for inserting real-time information: mean prediction error vs. fraction of revealed variables. Each method is presented at its best α value. The error that would be obtained by using thistorical data as a prediction is added for reference.

These states may either be purely spatial or more likely spatio-temporal configurations, depending on the underlying graph. Given a day-time observed configuration, the question is which fixed point (defined by its set of beliefs) is the most representative of such a sample which is simply given by a complete set[2] of observed traffic indexes (1), $\mathbf{x}^* = \{x_i^*, i \in \mathcal{V}\}$ and the associated probability $\mathbf{p}^*$. This is to be compared to the corresponding set of beliefs $\mathbf{b}^s = \{b_i^s, i \in \mathcal{V}\}$ of each fixed points s, with help of some distance $d(\mathbf{b}^s, \mathbf{p}^*)$. For each sample, the reference fixed point is the nearest one w.r.t. this distance. In practice, the complete enumeration of fixed points might be a difficult task with limited usefulness, since we are actually interested in the fixed points which can readily be attained. A natural way to proceed, from the algorithmic viewpoint, is to actually bias the convergence of BP in the "direction" of the sample, by substituting to the original ϕ's in the update rules

$$\phi_i^n(\tau_i) \stackrel{\text{def}}{=} (1 - \epsilon^n)\hat{p}_i(x_i) + \epsilon^n p_i^*(\tau_i) \qquad \forall i \in \mathcal{V}^*,$$

with $\epsilon < 1$, so that ϕ is recovered at the end of the BP convergence. With this guiding mechanism, we automatically select the fixed point closest to $\mathbf{x}^*$.

The experimental setting is as follows: 200 configurations are again randomly selected from the historical database, and associated BP fixed points are determined for different values of α, according to the procedure detailed above. The distortion is then defined as the mean over $\mathcal{V}$ of $|x_i^* - b_i^s(1)|$.

The results for SIouxFalls are plotted in Fig. 5, in parallel with the integrated reconstruction performance measure from previous section. The fixed points analysis yields coherent results with the reconstruction plots, in particular the same value of α yields the best reconstruction and minimizes the clustering distortion; this is clear for Sioux Falls data, but less for Paris region (not shown).

[2]which is actually possible only with artificial data where a complete information is available

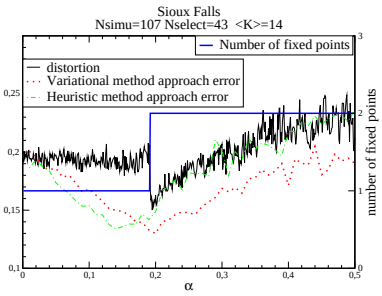

Fig. 5. Fixed point analysis for Sioux Falls network. The minimum clustering distortion coincide with the lowest prediction error of the variational method.

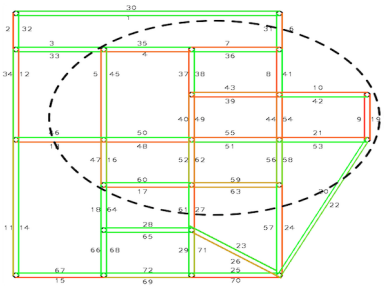

Fig. 6. The global traffic pattern of the second fixed point

V. Attempt at a synthesis

Both fixed points obtained in the BP approach on Sioux-Fall database can now be compared with cluster exemplars obtained with AP. The first BP fixed point has a 0.95 mean traffic index and corresponds to the free-flow AP exemplars. Fig. 6 provides illustrations of the global traffic state corresponding to the second fixed point, with identical color convention as in Section III. By comparison with Fig. 2, global structures of this fixed point appear to be similar with the congested cluster exemplars in the second optimal clustering solution, although the second BP fixed point seems to be shifted to higher congestion. To have more insight into this, we project all 72D index vectors and fixed points to 3D eigenspace using PCA in Fig. 7. We observe that the first and the second points are respectively located inside the free-flowing and severe congestion clusters. Notably, over 80% of congested links are shared between the second BP fixed point and the severe congestion cluster in the second sub-optimal clustering solution. In these two figures, most of congested links are located within a specific region (the oval of Fig. 6). This location consistency implies that links within the regions are more likely to be jammed together, hinting at some correspondences between results of off-line statistical analysis and stable states obtained with BP.

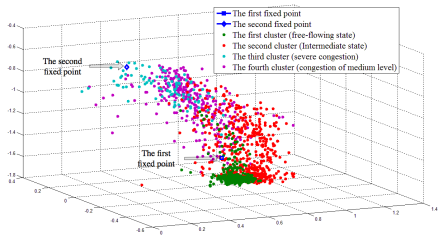

Fig. 7. Distribution of fixed points and data points of all four clusters

VI. Acknowledgements

This work was supported by the grant ANR-08-SYSC-017 from the French National Research Agency.

References

[1] R. Herring, A. Hofleitner, S. Amin, T. Nasr, A. Khalek, P. Abbeel, and A. Bayen, "Using mobile phones to forecast arterial traffic through statistical learning," in *89th Transportation Research Board Annual Meeting*, Washington D.C., January 10-14 2010.

[2] "REACT, Realizing Enhanced Safety and Efficiency in European Road Transport," `http://www.react-project.org/`.

[3] D. Chowdhury, L. Santen, and A. Schadschneider, "Statistical physics of vehicular traffic and some related systems," *Physics Report*, vol. 329, p. 199, 2000.

[4] A. Klar, R. Kuehne, and R. Wegener, "Mathematical models for vehicular traffic," *Surv. Math. Ind.*, vol. 6, p. 215, 1996.

[5] K. Nagel and M. Schreckenberg, "A cellular automaton model for freeway traffic," *J. Phys. I,2*, pp. 2221–2229, 1992.

[6] R. Chrobok, J. Wahle, and M. Schreckenberg, "Traffic forecast using simulations of large scale networks," in *Proceedings*, ser. Intell. Transport. Sys. Conf. Oakland(CA), USA: IEEE, August 25-29 2001.

[7] T. Guozhen, Y. Wenjiang, and H. Ding, "Traffic flow prediction based on generalized neural network," in *Proceedings*, ser. Intell. Transport. Sys. Conf. Washington, D.C. USA: IEEE, October 3-6 2004.

[8] W. Chun-Hsin, H. Jan-Ming, and D. Lee, "Travel-time prediction with support vector regression," *IEEE Trans. Intell. Transport. Syst.*, vol. 5, no. 4, p. 276, 2004.

[9] H. Kanoh *et al.*, "Short-term traffic prediction using fuzzy c-means and cellular automata in a wide-area road network," in *Proceedings of the 8th International*, ser. Conf. Intell. Transport. Sys. Vienna, Austria: IEEE, September 13-16 2005.

[10] Y. Kamarianakis and P. Prastacos, "Space-time modeling of traffic flow," *Comput. Geosci.*, vol. 31, no. 2, pp. 119–133, 2005.

[11] B. Ghosh, B. Basu, and M. O'Mahony, "Multivariate short-term traffic flow forecasting using time-series analysis," *Trans. Intell. Transport. Sys.*, vol. 10, no. 2, pp. 246–254, 2009.

[12] C. Furtlehner, J. Lasgouttes, and A. De La Fortelle, "A belief propagation approach to traffic prediction using probe vehicles," in *Proc. IEEE 10th Int. Conf. Intel. Trans. Sys.*, 2007, pp. 1022–1027.

[13] J. Pearl, *Probabilistic Reasoning in Intelligent Systems: Network of Plausible Inference*. Morgan Kaufmann, 1988.

[14] F. Marchal, "Contribution to dynamic transportation models," Ph.D. dissertation, University of Cergy-Pontoise, 2001.

[15] A. de Palma and F. Marchal, "Real cases applications of the fully dynamic METROPOLIS tool-box: an advocacy for large-scale mesoscopic transportation systems," *Networks and Spatial Economics*, vol. 2, no. 4, pp. 347–369, 2002.

[16] L. J. LeBlanc, E. K. Morlok, and W. Pierskalla, "An efficient approach to solving the road network equilibrium traffic assignment problem," *Transportation Research*, vol. 9, pp. 309–318, 1975.

[17] J.MacQueen, "Some methods for classification and analysis of multivariate observations," in *Proceedings of 5th Berkeley Symposium on Mathematical Statistics and Probability*, 1967.

[18] B. J.Frey and D. Dueck, "Clustering by passing messages between data points," *Science*, vol. 315, pp. 972–976, 2007.

[19] C. Furtlehner, J.-M. Lasgouttes, and A. Auger, "Learning multiple belief propagation fixed points for real time inference," *J. Phys. A*, vol. 389, no. 1, pp. 149–163, 2010.

[20] J. S. Yedidia, W. T. Freeman, and Y. Weiss, "Constructing free-energy approximations and generalized belief propagation algorithms," *IEEE Trans. Inform. Theory.*, vol. 51, no. 7, pp. 2282–2312, 2005.